Journal of the Iranian Chemical Society (2022) 19:2505–2517
https://doi.org/10.1007/s13738-021-02473-9

ORIGINAL PAPER

Influence of mesoporous carbon and silica structures as support on catalytic behavior of CMK-3 and MCM-41 modified Cu(II)-acetohydrazide in multicomponent organic reactions

Raziyeh Ghafouri-Nejad[1] · **Shabnam Rashidi**[1] · **Maryam Hajjami**[2]

Received: 14 September 2021 / Accepted: 2 December 2021 / Published online: 28 January 2022

Abstract

Cu(II)-acetohydrazide functionalized CMK-3 and MCM-41 mesoporous materials prepared by a simple, efficient and less expensive protocol. These catalysts are carefully characterized by SEM, XRD, TGA, FT-IR, EDX, ICP-OES and BET techniques. The obtained nanostructured compounds were also used as a green, efficient, heterogeneous and reusable catalytic systems for the synthesis of 2-amino-4-H-pyran and 2,4,5-trisubstituted imidazole derivatives. Also the results and behavior of the two catalysts were comparable in some cases. The synthesized nanocatalysts could be easily recovered from the reaction mixture and reused many times without significant loss of their catalytic activities.

✉ Maryam Hajjami
m.hajjami@basu.ac.ir; mhajjami@yahoo.com

[1] Department of Chemistry, Faculty of Science, Ilam University, P. O. Box: 69315516, Ilam, Iran

[2] Department of Organic Chemistry, Faculty of Chemistry, Bu-Ali Sina University, P. O. Box: 6517838683, Hamedan, Iran

Graphical abstract

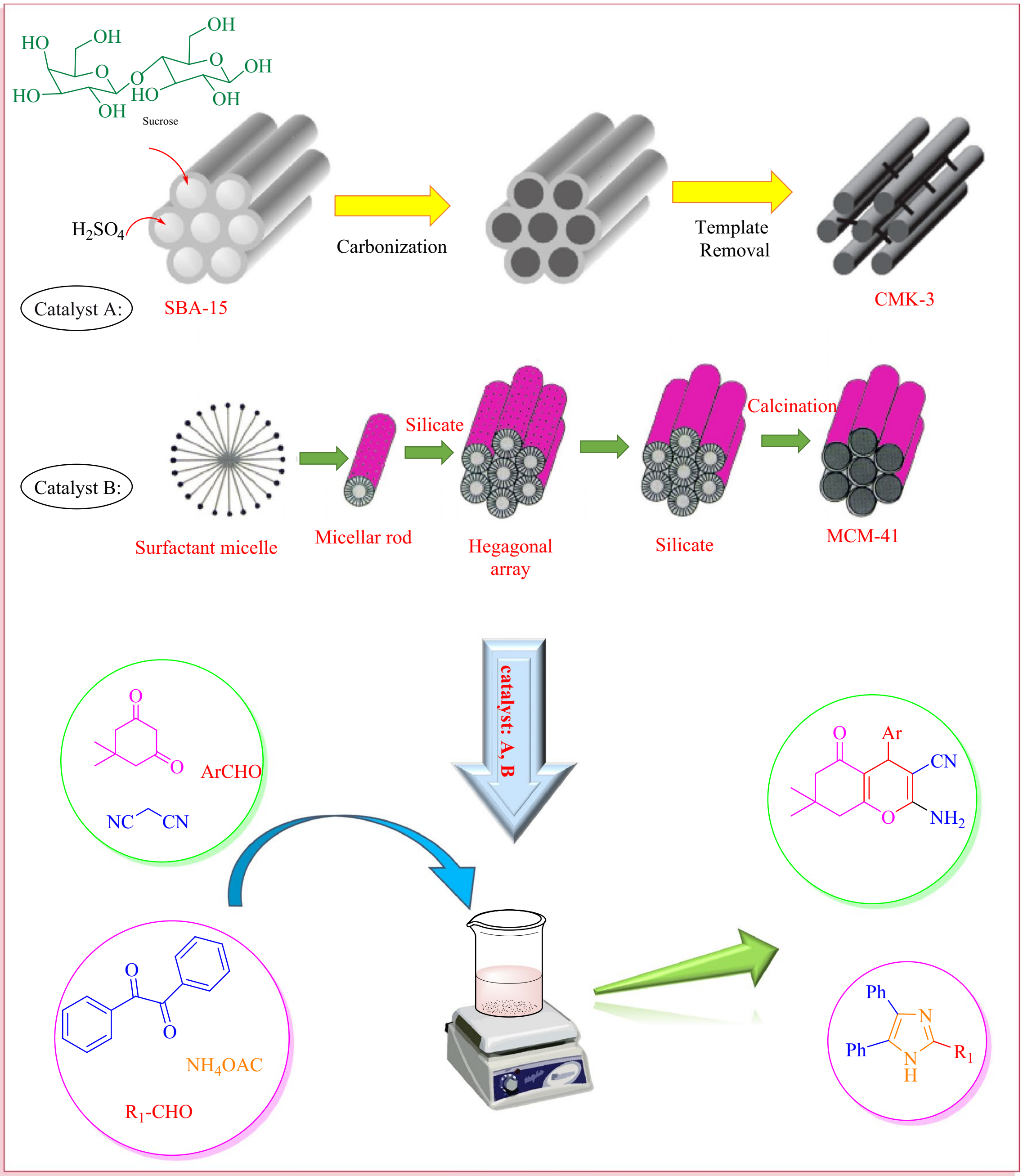

Keywords Acetohydrazide · CMK-3 · MCM-41 · Mesoporous · Multicomponent reactions · 2-Amino-4-H-pyran · Imidazole

Introduction

Mesoporous materials with unique properties, including high surface area, uniform pore size and high thermal stability, could employ for the synthesis of heterogeneous catalysts [1, 2]. Mesoporous materials have pore sizes in the range between 2 and 50 nm [3]. Mesoporous materials have many applications such as catalysis, drug delivery and adsorption [4]. Silicate and carbon materials are among the most important and widely used mesoporous materials [5]. The most well known of silicate mesoporous materials is the hexagonal MCM-41 with pore size 2–50 nm [6, 7].

In recent years, mesoporous carbon materials have received much attention due to their many applications. Applications of these materials include their use as solid surfaces for catalysts, electrodes and adsorbents for the purification of liquids and gases, substrates in chromatography columns and controlled drug delivery media. These materials have many advantages such as high specific surface area, uniform pore diameter, high pore volume, high thermal and chemical stability, and regular framework and excellent pore size distribution [8–11]. CMK-3 mesoporous carbon, which was synthesized using SBA-15 silica as the template and sucrose as the carbon source, is one of the most common and widely used ordered mesoporous carbon materials [10, 12].

Imidazoles are a five-membered aromatic heterocycle containing two nitrogen heteroatoms that play a key role in the structure of bioactive molecules [13]. Compounds containing imidazole have many medicinal properties and play an important role in biochemical processes [2]. Applications of imidazole derivatives include anti-inflammatory, anti-inflammatory, anti-tumor, anesthetic, anti-fungal, anti-parasitic and anti-bacterial. Many diaryl imidazole derivatives have also been identified as light-sensitive materials in photography, as inhibitors p38 MAP kinase, herbicides, and herbicides, and plant growth regulators [7, 14, 15].

There are numerous methods in the literature for the synthesis of imidazoles: condensation of 1,2–diones, aldehydes and ammonia in the presence of several catalysts such as ZnO [16], nano-aluminium nitride [13], GO–chitosan [14], MCM-41-nPr-NHSO$_3$H [2], ZrO$_2$-Al$_2$O$_3$ [15], Cu(I)-1,3-dimethylbarbituric acid modified SBA-15 [7] and FSM-16/CPTMS-Rh-Ni (II) [17].

2-Amino-4H-pyran compounds are an essential class of heterocyclic compounds that are of great importance due to their biological and medical properties [18]. These compounds are used as anti-tumor, anti-bacterial, anti-allergic, anti-cancer and anti-coagulant agents [18–20]. Besides, these compounds can be used to treat neurodegenerative diseases, including Alzheimer's, Huntington's, Parkinson's, HIV and Down syndrome [21, 22]. Some derivatives of these compounds are used in cosmetics and pigments as well as biodegradable chemicals [23]. 2-Amino-4H-pyrans were synthesized by condensation of aldehydes, malononitrile and β-dicarbonyl compounds. Literatures survey shows that several methods have been reported using various catalysts such as potassium phthalimide-N-oxyl [24], [MPIm][HSO$_4$]@SBA-15 [25], *L*-proline [26], [pyridine–SO$_3$H]Cl [27], nano-sized MgO [28], diamine-functionalized Fe$_3$O$_4$@SiO$_2$ [20] and HMS/Pr-Rh-Zr [29].

In this study, Cu(II)-acetohydrazide complexes are grafted on mesoporous MCM-41 and CMK-3 using chloropropyltriethoxysilane (CPTES) as linker to the surface. The resulting new material is applied as heterogeneous catalysts for the synthesis of 2-amino-4-H-pyran and 2,4,5-trisubstituted imidazole derivatives.

Experimental

Materials and instrumentation

All reagents and solvent used in this work were bought from Sigma-Aldrich and Merck chemical companies and used without further purification. IR spectra were recorded as KBr pellets on a VRTEX 70 model BRUKER FT-IR spectrophotometer. The thermogravimetric analysis (TGA) was used with a heating rate of 15 °C/min in air, and the samples were heated from room temperature to 800 °C. X-ray diffraction (XRD) patterns were recorded using a Cu Ka radiation source with wave length 1.54 Å. The particle size and morphology were examined by measuring SEM using FESEM-TESCAN. The elemental analysis of the samples was done by energy-dispersive X-ray spectroscopy (EDAX, TSCAN). The content of Cu was measured by inductively coupled plasma-optical emission spectrometry (ICP-OES).

Synthesis of CMK-3

The CMK-3 carbon was prepared according to the process described in the literature using SBA-15 as the hard template and sucrose as the carbon source. [30]. The mesoporous SBA-15 was prepared according to the previously reported procedure [7]. Typically, 1 g SBA-15 was added to a solution containing 1.25 g of sucrose and 0.14 g of H$_2$SO$_4$ in 5 g of H$_2$O. The resulting mixture was heated in an oven at 100 °C for 6 h and then 160 °C for another 6 h.

The silica sample, containing partially polymerized and carbonized sucrose, was treated again with 0.7 g of sucrose, 0.09 g of H$_2$SO$_4$ and 5 g of water and then heated at 100 °C and 160 °C. Then, the resulting composite was carbonized at 900 °C under N$_2$ flow for 5 h. Finally, the resulting solid was washed with 1 M NaOH solution two times to remove the silica template, filtered, washed with ethanol and dried at 100 °C for 4 h. Mesoporous carbon CMK-3 was obtained.

Synthesis of MCM-41

MCM-41 silica was prepared by using the hydrothermal method [31]. In this process 3.64 g (1 mol%) of CTAB and 1.2 g (3.01 mol%) of NaOH were solved in 108 mL of deionized water and mixed in a stainless steel autoclave, and then 241 g (9.8 mol%) of TEOS was added to the solution, which was stirred for 60 min at room temperature. Then, the sol was aged for 1 h and put in an oven at 110 °C during 96 h. After 96 h, the resulting white precipitate was filtered, washed with deionized water and 50 mL of ethanol. The resulting powder

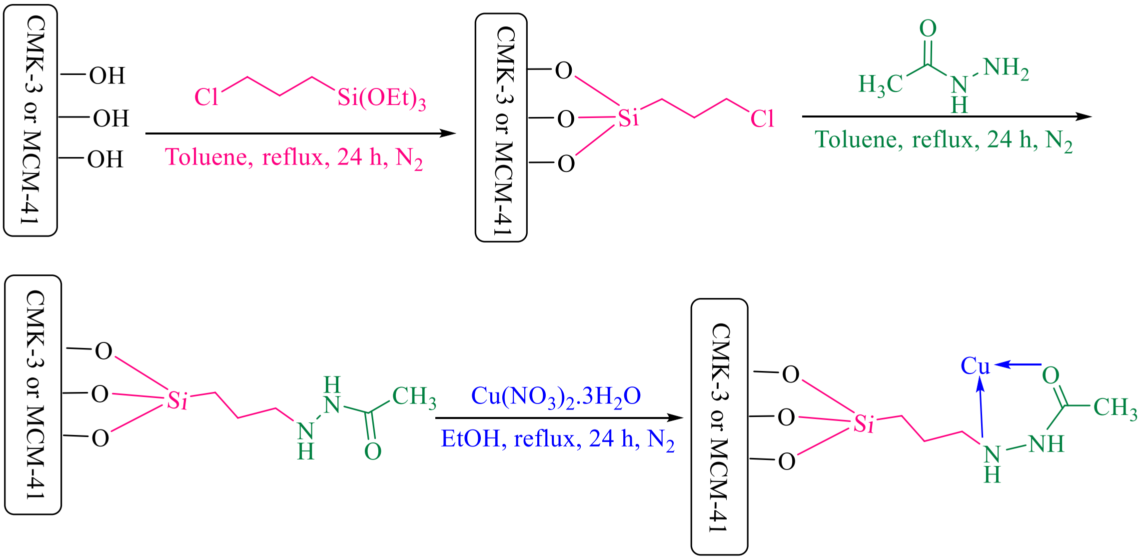

Scheme 1 Synthesis of Cu(II)-acetohydrazide supported CMK-3 (catalyst A) and Cu(II)-acetohydrazide supported MCM-41(catalyst B)

was dried at 80 °C for 2 h. Removal of the template was performed by calcination in air at 550 °C for 5 h (heating rate of 2 °C/min).

Synthesis of Cu(II)-acetohydrazide supported CMK-3 and Cu(II)-acetohydrazide supported MCM-41

Firstly, 3 ml 3-chloropropyltriethoxysilane was added dropwise to 1 g of vacuum-dried mesoporous dispersed in 100 mL of toluene under vigorous stirring and N_2 atmosphere. Then the reaction mixture was stirred under reflux condition for 24 h under N_2 atmosphere. Afterward, the resulting solid was filtered, washed with dichloromethane and dried at room temperature for 24 h to obtain chlorofunctionalized-MCM-41(MCM-41-nPr-Cl) or chlorofunctionalized-CMK-3 (CMK-3-nPr-Cl). Then acetohydrazide and chlorofunctionalized mesoporous with ratio 3:1 was added to absolute toluene in the presence of 1 ml of triethylamine (Et_3N) and refluxed at under N_2 atmosphere for 24 h. Then the mixture was filtered, washed with dichloromethane and dried at room temperature. Then $Cu(NO_3)_2.3H_2O$ was added to this sediment (with ratio 2:1) in ethanol, and mixture was stirred for 24 h refluxed under N_2 atmosphere. Finally the resulting product was washed with ethanol and dried at room temperature for 24 h to afford Cu(II)-acetohydrazide supported CMK-3(catalyst A) or Cu(II)-acetohydrazide supported MCM-41(catalyst B) (Scheme 1).

General procedure for preparation of 2-amino-4H-pyran derivatives

A mixture of malononitrile (1 mmol), aldehyde (1 mmol), dimedone and catalyst A (20 mg) or catalyst B (40 mg) in the water (3 ml) was stirred at 70 °C (catalyst A) or 90 °C (catalyst B) for the certain period of time. After completion of the reaction as indicated by TLC (n-hexane–acetone, 8:2), the catalyst was separated of the reaction by filtration and the mixture was washed with ethyl acetate. The organic product was isolated with ethyl acetate and dried after washing. For more purification the products were recrystallized in ethanol.

General procedure for the synthesis of 2,4,5-trisubstituted imidazole derivatives

For the synthesis of 2,4,5-trisubstituted imidazoles, a mixture of benzil (1 mmol), aromatic aldehyde (1 mmol), ammonium acetate (4.5 mmol) and catalyst A (30 mg) or catalyst B (20 mg) was heated in the oil bath at 100 °C for the appropriate time. The reaction was monitored by TLC. After completion of the reaction mixture was cooled to room temperature; ethyl acetate was added and filtered. The product was extracted with ethyl acetate, and the catalyst was separated by simple filtration and then recrystallized from ethanol to give pure substituted imidazole product.

Results and discussion

Catalyst preparation

Here in us describe the preparation of new heterogeneous catalysts A and B by functionalization of MCM-41 and CMK-3 with 3-chloropropyltriethoxysilane and subsequent immobilization of acetohydrazide on the chlorofunctionalized mesoporous. Then by adding $Cu(NO_3)_2.3H_2O$ the

Cu(II)-acetohydrazide supported CMK-3 (catalyst A) or Cu(II)-acetohydrazide supported MCM-41 (catalyst B) was synthesized.

Catalyst characterization

The catalysts have been characterized by some microscopic and spectroscopic techniques including Fourier transform infrared (FT-IR) spectroscopy, X-ray diffraction (XRD), thermogravimetric analysis (TGA), scanning electron microscopy (SEM), N_2 adsorption–desorption analysis (BET), energy-dispersive X-ray spectroscopy (EDX) and inductively coupled plasma atomic emission spectroscopy (ICP-OES).

The FT-IR spectra of CMK-3, CMK-3-nPr-Cl, CMK-3-nPr-acetohydrazid and CMK-3-nPr-acetohydrazide-Cu(II) samples are shown in Fig. 1.

The FT-IR spectrum of the CMK-3 is shown in Fig. 1a; in this spectrum, peaks of silica template were not observed indicating removal of SBA-15 hard template. The peak appeared at 1045 cm^{-1} has assigned to the vibrations of the C–O bond. The peaks appeared at 1400 cm^{-1} and 1632 cm^{-1} are related to the stretching vibrations of the C=C bands in the aromatic ring. Also, stretching vibrations of C–H bond were observed at 2853 cm^{-1} and 2923 cm^{-1} and OH group at 3439 cm^{-1} [32].

In the FT-IR spectra of CMK-3-nPr-Cl (Fig. 1b), the Si–O–Si bond, asymmetric stretching vibration and symmetric stretching vibration appear at 1088 cm^{-1} and 802 cm^{-1}, respectively. Also, C–H bending vibration appears at 2853 cm-1, in which the presence of the 3-chloropropyl silane was confirmed.

In the FT-IR spectra of CMK-3-nPr-acetohydrazid (Fig. 1c), the existence of the grafted acetohydrazide group is identified by C–N and C=O stretching vibration that appears at 1379 cm^{-1} and 1641 cm^{-1}, respectively, in which C–N band has been shifted to higher frequency (1384 cm^{-1}) and C=O band has been shifted to lower frequency (1637 cm^{-1}) in the CMK-3-nPr-acetohydrazide-Cu(II) (Fig. 1d), indicating the formation of Cu complex on surface of mesoporous carbon CMK-3.

The FT-IR spectra of MCM-41, MCM-41-nPr-Cl, MCM-41-nPr-acetohydrazid and MCM-41-nPr-acetohydrazide-Cu(II) samples are shown in Fig. 2.

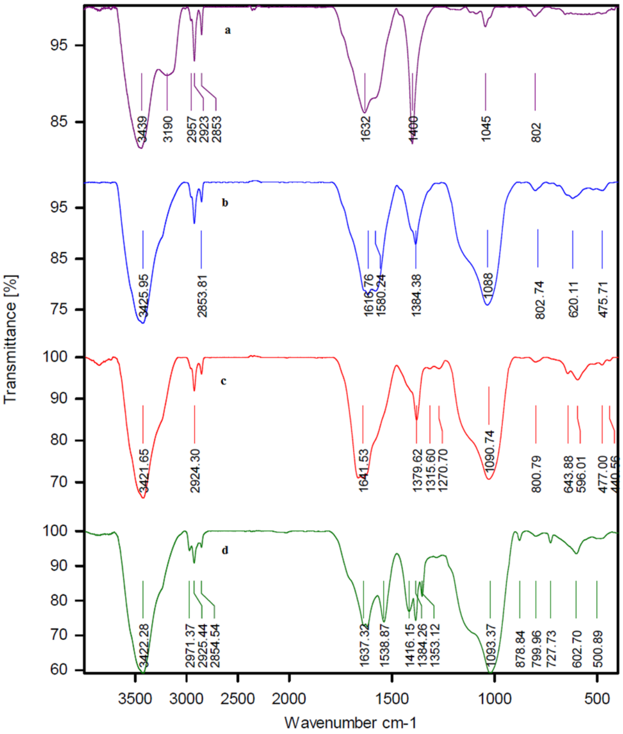

Fig. 1 The FT-IR spectra of **a** CMK-3, **b** CMK-3-nPr-Cl, **c** CMK-3-nPr-acetohydrazid and **d** CMK-3-nPr-acetohydrazide-Cu(II)

In the all spectra, the sharp peak at 1087 cm^{-1} can be attributed to the asymmetric stretching vibration of the Si–O–Si band and 814 cm^{-1} can be assigned to the symmetric stretching vibration of Si–O and a peak in 3430 cm^{-1} which are assigned to O–H band [31]. In the spectra of MCM-41-nPr-Cl (Fig. 1b), the C-H bending vibration appears at 2853 cm^{-1}, in which the presence of the 3-chloropropyl silane was confirmed. In the FT-IR spectra of MCM-41-nPr-acetohydrazid (Fig. 1c), the existence of the grafted acetohydrazide group is identified by C–N and C=O stretching vibration that appeared at 1383 cm^{-1} and 1634 cm^{-1}, respectively.

Figure 3 shows low-angle XRD patterns for CMK-3 and Cu(II)-acetohydrazide supported CMK-3 (catalyst A). The spectra of CMK-3 exhibit a diffraction peak (100) which indicates the sample has two-dimensional hexagonal mesoporous structure [32]. This shows clearly that the framework structure does not deteriorate seriously during treatment with chloropropyltriethoxysilane, and acetohydrazide, and $Cu(NO_3)_2.3H_2O$. Some loss in the intensity of the peak was observed after modification, providing further evidence of functionalization occurring mainly inside the mesopore pores.

Figure 4 shows low-angle XRD pattern for MCM-41-nPr-acetohydrazide-Cu(II). This pattern illustrates typical peaks corresponding to diffraction at (100), (110) and (200) plane of hexagonal phase described in the literature [31]. It is remarkably that the MCM-41 still holds the hexagonal mesoporous structure even after reacting with organic groups.

Figure 5 shows TGA curves of pristine CMK-3 and CMK-3-nPr-acetohydrazide-Cu(II). The results were confirmed by TGA data by showing 5% weight loss before 100 °C for CMK-3, which is due to desorption of physical absorption water on the surface of CMK-3. Secondly, the

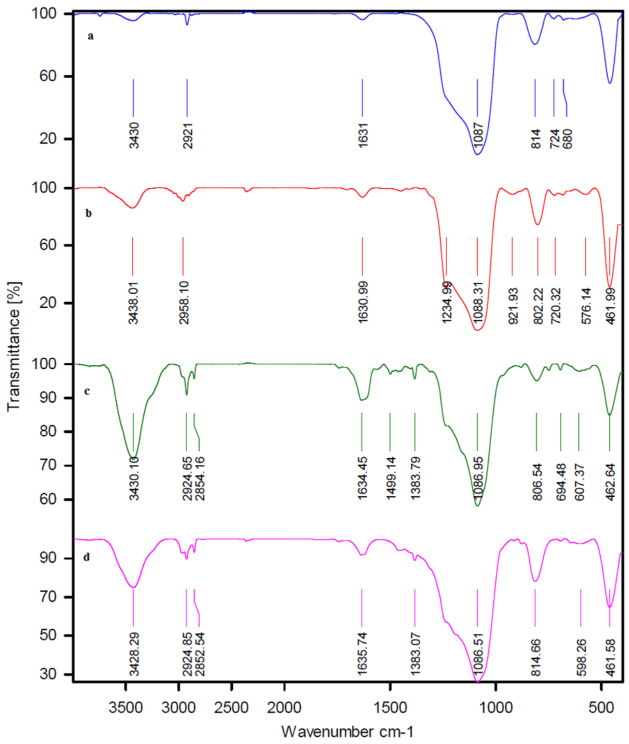

Fig. 2 The FT-IR spectra of **a** MCM-41, **b** MCM-41-nPr-Cl, **c** MCM-41-nPr-acetohydrazide and **d** MCM-41-nPr-acetohydrazide-Cu(II)

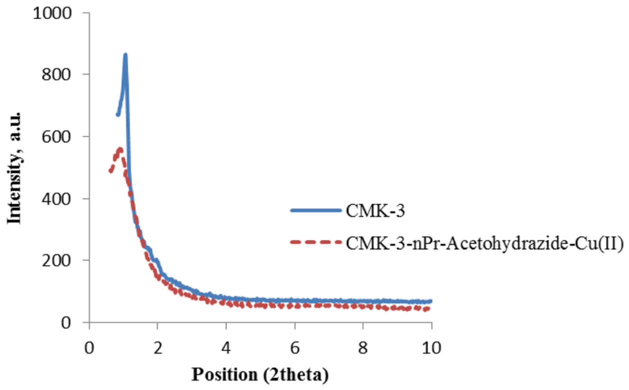

Fig. 3 The XRD patterns of CMK-3 and CMK-3-nPr-acetohydrazide-Cu(II)

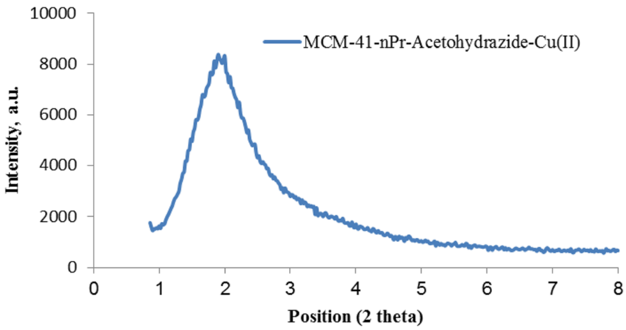

Fig. 4 The XRD pattern of MCM-41-nPr-acetohydrazide-Cu(II)

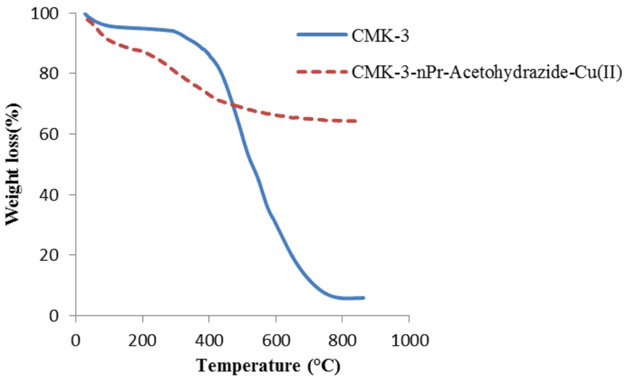

Fig. 5 TGA diagram of CMK-3 and CMK-3-nPr-acetohydrazide-Cu(II)

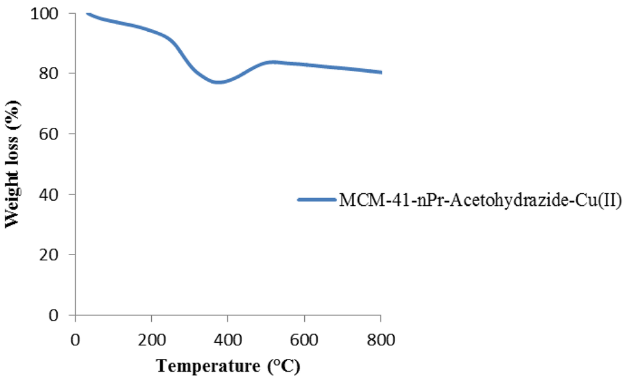

Fig. 6 TGA curve of MCM-41-nPr-acetohydrazide-Cu(II)

weight loss between 300 and 650 °C is due to the combustion of CMK-3 [33]. In TGA curve of the CMK-3-nPr-acetohydrazide-Cu(II) a weight loss (10%) before 100 °C is due to the trapped water, and also a weight loss about 20% from 200 to 600 °C is attributed to the decomposition of immobilized organic spaces on the surface of CMK-3.

Figure 6 shows TGA curve of MCM-41-nPr-acetohydrazide-Cu(II). In TGA curve of the MCM-41-nPr-acetohydrazide-Cu(II) a weight loss (10%) before 200 °C is due to the trapped water, and also a weight loss about 18% from 150 to 370 °C is attributed to the decomposition of immobilized organic groups on the surface of MCM-41 [31].

The N_2 adsorption–desorption isotherms for CMK-3, CMK-3-nPr-acetohydrazide-Cu(II) (catalyst A) and MCM-41-nPr-acetohydrazide-Cu(II) (catalyst B) are shown in Figs. 7 and 8. The isotherms of this adsorbent are of type-IV curves according to the IUPAC classification, indicating the characterization of the ordered mesoporous material [8].

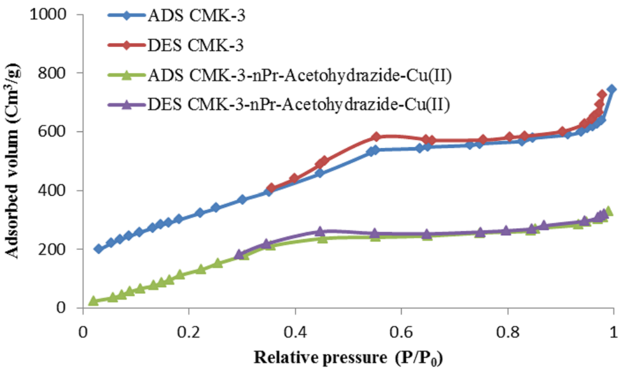

Fig. 7 Nitrogen adsorption–desorption isotherms of CMK-3 and CMK-3-nPr-acetohydrazide-Cu(II)

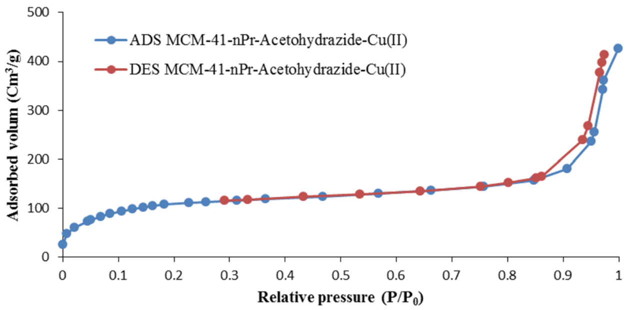

Fig. 8 Nitrogen adsorption–desorption isotherms of MCM-41-nPr-acetohydrazide-Cu(II)

The surface area (S_{BET}), the average pore diameter (D_{BJH}) and the total pore volumes (V_{total}) of synthesized samples are summarized in Table 1. The surface area and pore volume of CMK-3 are high (1162 cm^2) which is typical of mesoporous materials. After functionalization, a decrease in the S_{BET}, D_{BJH} and V_{total} was observed that can be easily interpreted due to the fact that the presence of pendant group on the pour surface partially blocks the adsorption of nitrogen molecules. In addition, obtained results revealed that the surface area and pore volume of modified CMK-3 are higher than modified MCM-41.

SEM images of the CMK-3-nPr-acetohydrazide-Cu(II) and MCM-41-nPr-acetohydrazide-Cu(II) are shown in Fig. 9. The image CMK-3-nPr-acetohydrazide-Cu(II) indicated maintains a rod-like structures CMK-3 carbon particles [34]. Also, the SEM image confirms that MCM-41-nPr-acetohydrazide-Cu(II) has regular and spherical morphology [31].

Table 1 Pore structure parameters of synthesized materials obtained by nitrogen adsorption–desorption analysis

Sample name	S_{BET} (m^2 g^{-1})	V_{total} (cm^3 g^{-1})	D_{BJH} (nm)
CMK-3-nPr-acetohydrazide-Cu(II)	370	0.91	1.7
MCM-41-nPr-acetohydrazide-Cu(II)	190	0.62	1.29

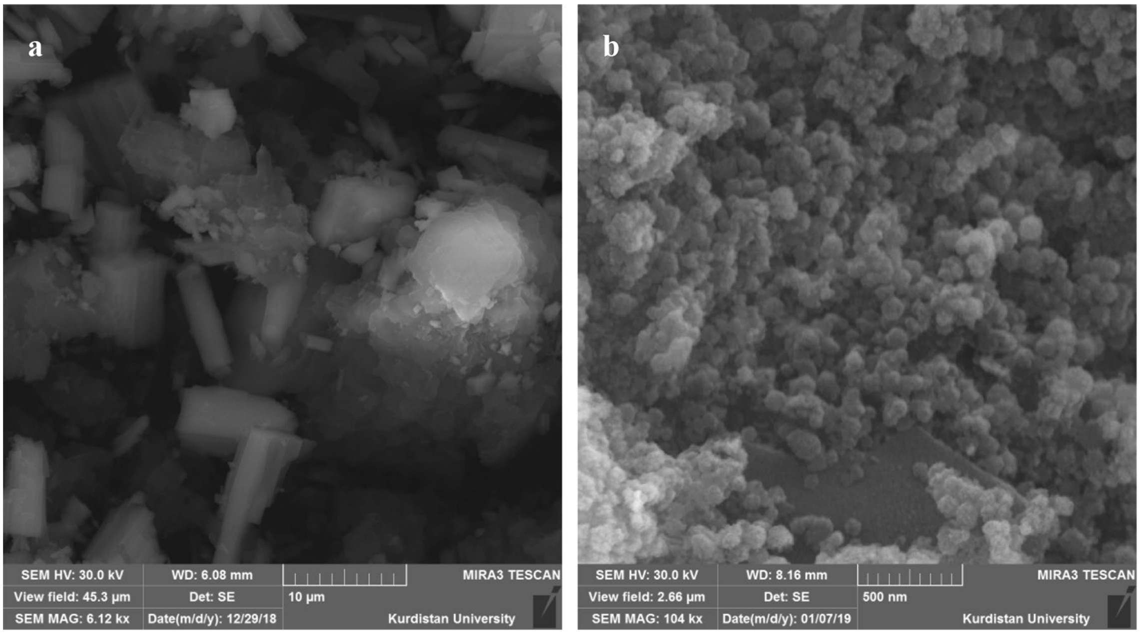

Fig. 9 The scanning electron microscopy (SEM) images of **a** CMK-3-nPr-acetohydrazide-Cu(II) and **b** MCM-41-nPr-acetohydrazide-Cu(II)

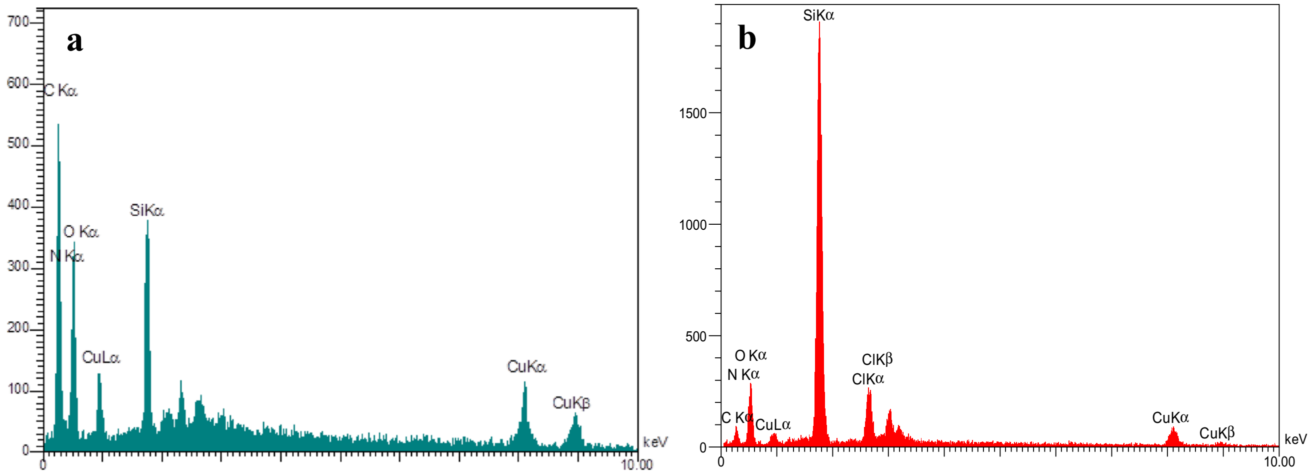

Fig. 10 EDS for **a** CMK-3-nPr-acetohydrazide-Cu(II) (catalyst A) and **b** MCM-41-nPr-acetohydrazide-Cu(II) (catalyst B)

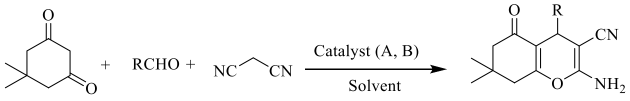

Scheme 2 Synthesis of 2-amino-4H-pyran derivatives

As shown in Fig. 10, the energy-dispersive X-ray spectrum (EDS) for the catalyst A and catalyst B determined the presence of C, N, O, Si and Cu species in the catalysts.

Based on inductively coupled plasma atomic emission spectroscopy (ICP-AES), the amount of Cu in the Cu(II)-acetohydrazide supported CMK-3 is 0.65 mol/g and in the Cu(II)-acetohydrazide supported MCM-41 is 0.61 mol/g.

Catalytic study

After synthesis and characterization of the catalysts, we first investigated the catalytic activities of CMK-3-acetohydrazide-Cu(II) and MCM-41-acetohydrazide-Cu(II) for the synthesis of 2-amino-4H-pyran derivatives (Scheme2). In order to optimize the reaction conditions, the reaction of 4-chlorobenzaldehyde (1 mmol), malononitrile (1 mmol) and dimedone was selected as a model reaction. Then, influence of solvent, temperature and amount of each catalyst on the outcome of reaction has been investigated (Table 2).

In order to choose the reaction media, different solvents such as EtOH, EtOH:H_2O mixture (1:1 ratio), ethyl acetate, CH_3CN and H_2O were used (Table 2, entries 1–5) and the best results were obtained in H_2O using 30 mg of catalyst A and 40 mg of catalyst B (Table 2, entry 5). Also, the effect of temperature was examined (Table 2, entries 5–7) and the best results were obtained at 70 °C for catalyst A and 90 °C for catalyst B (Table 2, entry 5).

After optimization of the reaction parameters, a variety of aromatic aldehydes with malononitrile and dimedone were employed as substrates for the synthesis of 2-amino-4H-pyran derivatives in the presence of MCM-41-acetohydrazide-Cu(II) and CMK-3-acetohydrazide-Cu(II) for the appropriate time in moderate to good yields. The results of this study are summarized in Table 3.

Also, the catalytic activities of MCM-41-acetohydrazide-Cu(II) and CMK-3-acetohydrazide-Cu(II) were studied in the preparation of tri-substituted imidazole derivatives (Scheme 3). To examine the optimal reaction conditions, the reaction of benzil (1 mmol), 4-chlorobenzaldehyde (1 mmol)

Table 2 Optimization of the synthesis of 2-amino-4H-pyrans conditions[a]

Entry	Solvent	Catalyst (mg) A/B	Temp.(°C) A/B	Yield (%)[b] A/B
1	EtOH	30/40	70/90	60/72
2	Ethyl acetate	30/40	70/90	45/85
3	CH_3CN	30/40	70/90	37/75
4	EtOH:H_2O	30/40	70/90	65/75
5	**H_2O**	**30/40**	**70/90**	**94[c]/95[c]**
6	H_2O	30/40	50/75	47/80
7	H_2O	30/40	25/50	34/65
8	H_2O	20/30	70/90	65/88
9	H_2O	10/20	70/90	60/85
10	H_2O	5/10	70/90	48/80

[a] Reaction conditions: 4-chlorobenzaldehyde (1 mmol), malononitrile (1 mmol), dimedone (1 mmol), time 10 min for catalyst A and 20 min for catalyst B

[b] purification by preparative TLC

[c] Isolated yield

Table 3 The synthesis of 2-amino-4H-pyrans using catalyst A and B[a]

Entry	Aldehyde	Product	Time (min) A/B	Yield (%)[b] A/B	M.p (M.p) [ref.]
1	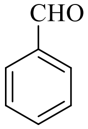	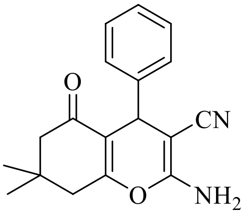	30/35	95/89	223–226 (227–228) [35]
2	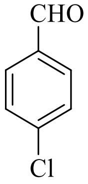	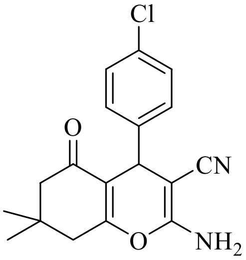	10/20	94/95	207–209 (209–210) [36]
3	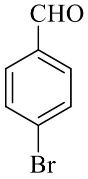	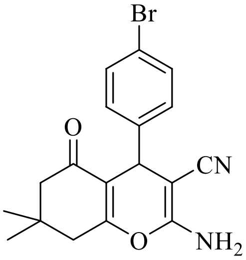	20/40	93/93	196–199 (197–199) [35]
4	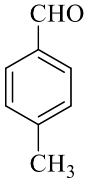	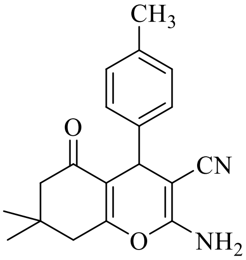	25/45	91/88	208–210 (209–211) [23]
5	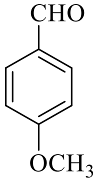	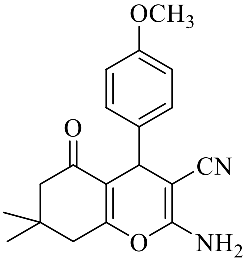	20/60	92/93	195–197 (197–199) [37]
6	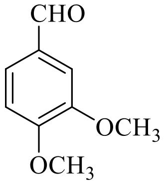	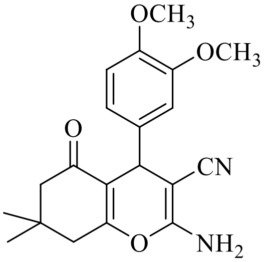	20/20	91/95	159–161 (158–160) [38]

Table 3 (continued)

Entry	Aldehyde	Product	Time (min) A/B	Yield (%)^b A/B	M.p (M.p) [ref.]
7	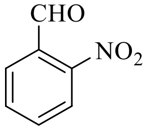	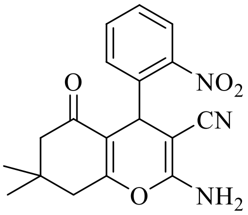	25/50	93/89	218–220 (220–221) [37]
8	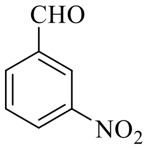	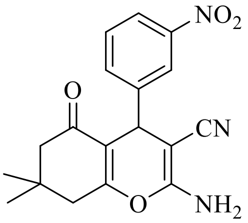	30/50	93/90	205–207 (206–209) [37]
9	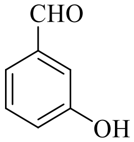	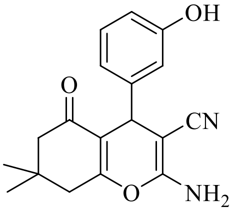	35/40	93/95	220–221 (220–221) [36]
10	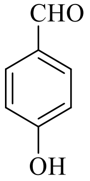	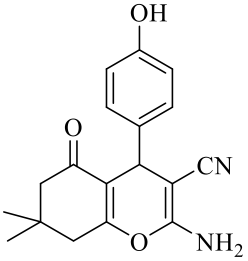	20/25	94/96	205–206 (205–206) [37]

[a] Reaction conditions: aldehydes (1 mmol), malononitrile (1 mmol) and dimedone (1 mmol), catalyst A (30 mg) and catalyst B (40 mg) in water at 70 °C for catalyst A and 90 °C for catalyst B

[b] Isolated yield

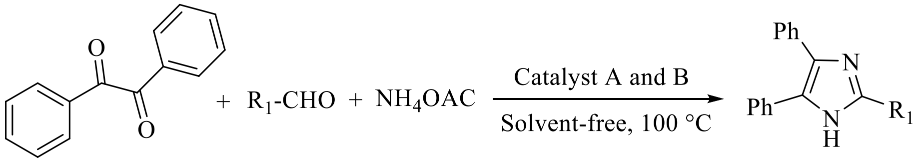

1a-1j

Scheme 3 Synthesis of tri-substituted imidazole derivatives

and ammonium acetate (5 mmol) was selected as a model reaction. The effects of various parameters such as temperature, solvent and amount of catalysts were considered in the model reaction (Table 4). As shown in Table 4, the best conditions were obtained for the catalyst, 30 mg of catalyst A (Table 4, entry 4) and 20 mg of catalyst B (Table 4, entry 9) in solvent-free at 100 °C.

After optimization of the reaction condition, the various aromatic aldehydes with benzil and ammonium acetate have been described in optimum condition and tri-substituted imidazole derivatives were obtained in excellent yields as shown in Table 5.

Table 4 Optimization of the synthesis of tri-substituted imidazoles conditions[a]

Entry	Solvent	Catalyst (mg) A/B	Temp.(°C) A / B	Yield (%)[b] A / B
1	EtOH	30/50	78/78	**- / -**
2	Ethyl acetate	30/50	77/77	**- / -**
3	H_2O	30/50	100/100	25/75
4	**Solvent-free**	**30**/50	**100**/100	**97**/90
5	Solvent-free	30/50	120/120	95/90
6	Solvent-free	30/50	80/80	80/85
7	Solvent-free	35/40	100/100	94/90[c]
8	Solvent-free	20/30	100/100	55/93
9	**Solvent-free**	10/**20**	100/**100**	45/**98**
10	Solvent-free	5/10	100/100	38/88

[a] Reaction conditions: 4-chlorobenzaldehyde (1 mmol), benzil (1 mmol), ammonium acetate (5 mmol), time 65 min for catalyst A and 90 min for catalyst B

[b] purification by preparative TLC

[c] Isolated yield

Reusability and recycling of the catalyst

Reusability and recyclability of the catalyst A and catalyst B were examined through reaction of 4-chlorobenzaldehyde, malononitrile and dimedone as a model reaction. After completion of the reaction, the reaction mixture was cooled to room temperature and dissolved in ethyl acetate. Then, the catalysts A and B were separated by simple filtration for subsequent experiments to investigate their reusability at the same reaction conditions. The results showed that catalysts are stable in reaction media and can be reused several times without significant loss of their catalytic activity (Fig. 11).

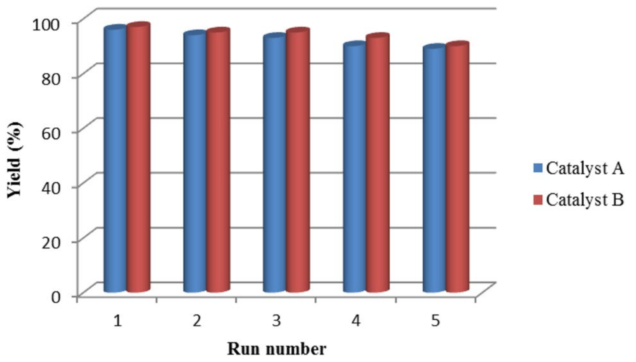

Fig. 11 Reusability and recycling of the catalyst A or catalyst B for the synthesis of 2-amino-4H-pyran

Comparison of the catalyst

In order to indicate the catalytic activities catalysts A and B comparison with other reported catalysts, we compared the results for the synthesis of 2-amino-4H-pyran in the presence of described catalysts with previously reported methods in the literature. The results summarized in Table 6 show that our catalysts afford short reaction time and higher yield than other catalysts.

Conclusions

In this study, Cu(II)-acetohydrazide supported on CMK-3 and MCM41 was successfully prepared as green, efficient and reusable catalysts for the synthesis of 2-amino-4-H-pyran and 2,4,5-trisubstituted imidazole derivatives. Catalytic application of these nano catalysts was investigated in synthesis of 2-amino-4-H-pyran and

Table 5 The synthesis of tri-substituted imidazoles using catalyst A and B[a]

Entry	Aldehyde	Product	Time (min) A/B	Yield (%)[b] A/B	M.p (M.p) [ref.]
1	C_6H_5	1a	70/85	91/88	272–274 [7]
2	$4\text{-}ClC_6H_5$	1b	65/90	97/98	258–260 [7]
3	$4\text{-}BrC_6H_5$	1c	95/155	96/94	248–250 [7]
4	$4\text{-}CH_3C_6H_5$	1d	70/85	95/96	226–229 [16]
5	$4\text{-}OCH_3C_6H_5$	1e	120/135	94/89	223–225 [16]
6	$3,4\text{-}(OCH_3)_2C_6H_5$	1f	150/180	95/90	211–213 [7]
7	$2\text{-}NO_2C_6H_5$	1 g	135/195	92/93	234–236 [39]
8	$3\text{-}NO_2C_6H_5$	1 h	120/265	91/93	309–311 [13]
9	$3\text{-}OHC_6H_5$	1i	40/145	94/90	259–261 [14]
10	$4\text{-}OHC_6H_5$	1j	60/130	91/92	120–122 [16]

[a]Reaction conditions: aldehydes (1 mmol), benzyl (1 mmol), ammonium acetate (5 mmol), catalyst A (30 mg) and catalyst B (20 mg) and solvent-free at 100 °C

[b]Isolated yield

Table 6 The comparison result of synthesis of 2-amino-4-(4-chlorophenyl)-4H-pyran by using formerly reported catalysts

Entry	Catalyst	Conditions	Time (min)	Yield (%)	Ref
1	DABCO	H_2O/Reflux	120	94	[19]
2	*L*-proline	EtOH/Reflux	90	87	[26]
3	Urea(4.8)/SBA-15	solvent-less /40 °C	240	98	[40]
4	IL-HSO_4@SBA-15	H_2O/45 °C	120	90	[25]
5	γ-Fe_2O_3 DMNPs	H_2O/r.t	300	90	[22]
6	CMK-3@acetohydrazide@Cu(II)	H_2O/70 °C	10	94	This work
7	MCM-41@acetohydrazide@Cu(II)	H_2O/90 °C	20	95	This work

2,4,5-trisubstituted imidazole derivatives. In the case 2-amino-4-H-pyran use of smaller amounts of CMK-3 catalyst, lower temperature and time compared with another catalytic system have been required. But for imidazole synthesis the less amount of MCM-41 catalyst was needed. In another hand for Cu(II)-acetohydrazide-CMK-3, although the amount of catalyst was higher, but reactions took less time. N_2 adsorption–desorption revealed the surface area and pore volume of modified CMK-3 are higher than modified MCM-41. TGA results confirm weight loss due to the decomposition of immobilized organic groups on the surface of MCM-41 and CMK is the same. The advantages of this protocol are the use of commercially available, cheap, the simple methodology, practicability, using water or solvent-free condition for organic reactions, easy of product isolation, recyclable and reusable catalyst, short reaction times and high product yields.

Supplementary Information The online version contains supplementary material available at https://doi.org/10.1007/s13738-021-02473-9.

Acknowledgements The authors acknowledge Ilam University, Ilam, Iran, and Bu Ali Sina University, Hamedan, Iran, for financial support of this work.

References

1. M. Khanmoradi, M. Nikoorazm, A. Ghorbani-Choghamarani, Appl. Organomet. Chem. **31**, e3693 (2017)
2. A. Ghorbani-Choghamarani, F. Ghorbani, Z. Yousofvand, G. Azadi, J. Porous Mater. **22**, 665 (2015)
3. M. Nikoorazm, A. Ghorbani-Choghamarani, M. Khanmoradi, RSC Adv. **6**, 56549 (2016)
4. T. Tamoradi, A. Ghorbani-Choghamarani, M. Ghadermazi, H. Veisi, Solid State Sci. **91**, 96 (2019)
5. J. Lee, J. Kim, T. Hyeon, Adv. Mater. **18**, 2073 (2006)
6. Z. Hamzah, N. Narawi, H.M. Rasid, A.N.M. Yusoff, Malays. J. Anal. Sci. **16**, 290 (2012)
7. M. Hajjami, F. Ghorbani, Z. Yousofvand, Appl. Organomet. Chem. **31**, e3843 (2017)
8. L. Hu, S. Dang, X. Yang, J. Dai, Microporous Mesoporous Mater. **147**, 188 (2012)
9. N.T. Thao, VNU, J. Sci. Nat. Sci. Technol. **27**, 259 (2011)
10. X. Wang, S. Wu, Z. Li, X. Yang, H. Su, J. Hu, Q. Huo, J. Guan, Q. Kan, Microporous Mesoporous Mater. **221**, 58 (2016)
11. R. Ghafouri-Nejad, M. Hajjami, React. Kinet. Mech. Catal. **129**, 371 (2020)
12. X. Xu, Z. Fan, X. Yu, S. Ding, D. Yu, X.W. Lou, Adv. Energy Mater. **4**, 1400902 (2014)
13. M. Hajjami, A. Ghorbani-Choghamarani, Z. Yousofvand, M. Norouzi, J. Chem. Sci. **127**, 1221 (2015)
14. A. Maleki, R. Paydar, RSC Adv. **5**, 33177 (2015)
15. N. Thimmaraju, S.M. Shamshuddin, RSC Adv. **6**, 60231 (2016)
16. K. Bahrami, M.M. Khodaei, A. Nejati, Monatshefte für Chemie-Chem. Mon. **142**, 159 (2011)
17. F. Gholamian, M. Hajjami, A.M. Sanati, Silicon **12**, 2121 (2020)
18. S. Tabassum, S. Govindaraju, M.A. Pasha, Ultrason. Sonochemistry **24**, 1 (2015)
19. D. Tahmassebi, J.A. Bryson, S.I. Binz, Synth. Commun. **41**, 2701 (2011)
20. A. Maleki, R. Ghalavand, R. Firouzi Haji, Appl. Organomet. Chem. **32**, e3916 (2018)
21. H. Hu, F. Qiu, A. Ying, J. Yang, H. Meng, Int. J. Mol. Sci. **15**, 6897 (2014)
22. S. Rostamnia, A. Nuri, H. Xin, A. Pourjavadi, S.H. Hosseini, Tetrahedron Lett. **54**, 3344 (2013)
23. D. Kumar, V.B. Reddy, S. Sharad, U. Dube, S. Kapur, Eur. J. Med. Chem. **44**, 3805 (2009)
24. M.G. Dekamin, M. Eslami, A. Maleki, Tetrahedron **69**, 1074 (2013)
25. S. Rostamnia, A. Hassankhani, H.G. Hossieni, B. Gholipour, H. Xin, J. Mol. Catal. A Chem. **395**, 463 (2014)
26. F. Behbahani, Gazi Univ. J. Sci. **28**, 387 (2015)
27. M.A. Zolfigol, A. Khazaei, A.R. Moosavi-Zare, J. Afsar, V. Khakyzadeh, O. Khaledian, J. Chin. Chem. Soc. **62**, 398 (2015)
28. D. Kumar, V.B. Reddy, B.G. Mishra, R. Rana, M.N. Nadagouda, R.S. Varma, Tetrahedron **63**, 3093 (2007)
29. S. Abdolahi, M. Hajjami, F. Gholamian, Res. Chem. Intermed. **47**, 1883 (2021)
30. J. He, K. Ma, J. Jin, Z. Dong, J. Wang, R. Li, Microporous Mesoporous Mater. **121**, 173 (2009)
31. M. Hajjami, Z. Shirvandi, Z. Yousofvand, J. Porous Mater. **24**, 1461 (2017)
32. S. Dorbes, C. Pereira, M. Andrade, D. Barros, A. Pereira, S. Rebelo, J. Araújo, J. Pires, A. Carvalho, C. Freire, Microporous Mesoporous Mater. **160**, 67 (2012)
33. L. Zeng, C. Deng, C. Zheng, H. Qiu, Q. Qian, Q. Chen, M. Wei, Mater. Res. Bull. **71**, 42 (2015)
34. M. Anbia, R. Dehghan, J. Environ. Sci. **26**, 1541 (2014)
35. A. Mobinikhaledi, H. Moghanian, M. Ghanbari, Appl. Organomet. Chem. **32**, e4108 (2018)

36. S.S. Katkar, M.K. Lande, B.R. Arbad, S.T. Gaikwad, Chin. J. Chem. **29**, 199 (2011)
37. O.H. Qareaghaj, S. Mashkouri, M.R. Naimi-Jamal, G. Kaupp, RSC Adv. **4**, 48191 (2014)
38. S. Zavar, Arab. J. Chem. **10**, S67 (2017)
39. Y. Zhang, Z. Zhou, Prep. Biochem. Biotechnol. **43**, 189 (2013)
40. J.N. Appaturi, M.R. Johan, R.J. Ramalingam, H.A. Al-Lohedan, Microporous Mesoporous Mater. **256**, 67 (2018)